Applied Catalysis B: Environmental 117–118 (2012) 49–58

Contents lists available at SciVerse ScienceDirect

Applied Catalysis B: Environmental

journal homepage: www.elsevier.com/locate/apcatb

Sulfur poisoning and regeneration of the Ag/γ-Al_2O_3 catalyst for H_2-assisted SCR of NO_x by ammonia

Dmitry E. Doronkin[a,*], Tuhin Suvra Khan[b], Thomas Bligaard[c], Sebastian Fogel[a,d], Pär Gabrielsson[d], Søren Dahl[a]

[a] Center for Individual Nanoparticle Functionality (CINF), Department of Physics, Technical University of Denmark, Fysikvej 307, 2800 Kgs. Lyngby, Denmark
[b] Center of Atomic-scale Materials Design (CAMD), Department of Physics, Technical University of Denmark, Fysikvej 307, 2800 Kgs. Lyngby, Denmark
[c] SUNCAT Center for Interface Science and Catalysis, SLAC National Accelerator Laboratory, Menlo Park, CA 94025, USA
[d] Haldor Topsøe A/S, Nymøllevej 55, 2800 Kgs. Lyngby, Denmark

ARTICLE INFO

Article history:
Received 1 November 2011
Received in revised form
27 December 2011
Accepted 3 January 2012
Available online 9 January 2012

Keywords:
Ag/Al_2O_3
SO_2
NO_x SCR
Poisoning
Regeneration

ABSTRACT

Sulfur poisoning and regeneration mechanisms for a 2% Ag/γ-Al_2O_3 catalyst for the H_2-assisted selective catalytic reduction of NO_x by NH_3 are investigated. The catalyst has medium sulfur tolerance at low temperatures, however a good capability of regeneration at 670 °C under lean conditions when H_2 is present. These heating conditions can easily be established during soot filter regeneration. Furthermore, two types of active sites could be identified with different regeneration capabilities, namely finely dispersed Ag and larger Ag nanoparticles. The most active sites are associated with the finely dispersed Ag. These sites are irreversibly poisoned and cannot be regenerated under driving conditions. On the other hand the larger Ag nanoparticles are reversibly poisoned by direct SO_x adsorption. The interpretation of the data is supported by DFT calculations.

1. Introduction

Selective catalytic reduction (SCR) is the leading NO_x control technique for diesel vehicles with ammonia used as a reductant. Commonly used catalysts are vanadia-based catalysts and Cu and Fe-containing zeolites. However, none of the systems demonstrate high thermal durability together with a good activity throughout the broad temperature region from 150 to 550 °C which is needed for vehicle applications [1]. Therefore, research of novel non-toxic, inexpensive and durable catalytic systems for NH_3-SCR is still an important focus area.

Recently two research groups suggested to use Ag/Al_2O_3, which is a well-known catalyst for NO_x SCR by hydrocarbons (HC-SCR), for SCR of NO_x by ammonia or urea with co-feeding hydrogen, resulting in nearly 90% NO_x conversion at temperatures as low as 200 °C [2,3]. Still, one of the major obstacles for the application of Ag/Al_2O_3 for NO_x SCR by ammonia is its rather poor sulfur tolerance [4]. A catalyst of 2% Ag/Al_2O_3 demonstrated a decrease in H_2-assisted NO_x conversion by urea from 50% to 30% after 20 h on stream in the presence of 50 ppm SO_2 at 250 °C. This is a rather good result considering the very high GHSV = 380,000 h^{-1} in the tests. However, the large amount of hydrogen (0.5%, 5:1 H_2:NO) used in this study is probably unacceptable for application in diesel vehicles because such a large consumption of hydrogen leads to a high "fuel penalty" [5].

A significant amount of data on sulfur tolerance of Ag/Al_2O_3 catalysts exists for NO_x SCR by hydrocarbons. Meunier and Ross [6] observed strong deactivation of a 1.2% Ag/Al_2O_3 catalyst for propene-SCR by 100 ppm SO_2 in the feed. It is noteworthy that the authors were able to recover most of the catalyst activity by treatment in 10% H_2/Ar at 650 °C or heating in the reaction mixture at 750 °C. Park and Boyer [7] compared the catalytic behavior of 2% and 8% Ag/Al_2O_3 catalysts in the presence of SO_2 and concluded that high Ag loadings may be preferential for making a sulfur tolerant catalyst. The authors demonstrated prominent activation of 8% Ag/Al_2O_3 by SO_2 in the feed and ascribed that to the formation of a very active silver sulfate phase.

When estimating the SO_2 tolerance of Ag/Al_2O_3 catalysts attention should be given also to the process temperature. Satokawa et al. [8] showed a clear dependence of the propane-SCR temperature on the deactivation degree with permanent catalyst deactivation at $T < 500$ °C and furthermore the ability to partially regenerate the catalyst by heating to 600 °C, even without removing low amounts (1 ppm) of SO_2 from the feed. Further studies [8] of sulfation-regeneration mechanisms included obtaining SO_2 TPD profiles and

* Corresponding author. Tel.: +45 4525 3275.
E-mail addresses: dmdo@fysik.dtu.dk, dmitriy.doronkin@gmail.com (D.E. Doronkin).

0926-3373/$ – see front matter © 2012 Elsevier B.V. All rights reserved.
doi:10.1016/j.apcatb.2012.01.002

attribution of peaks to different types of adsorbed SO_2, bound to Ag and alumina. The catalyst regeneration temperature was lower than any of the SO_2 desorption peaks, observed in the study, which did not allow drawing a clear conclusion about the deactivation and regeneration mechanisms.

Breen et al. [9] also demonstrated a drastic dependence of the catalyst degree of poisoning on the temperature of NO_x SCR by octane and toluene. The following was observed; at low temperatures (<235 °C) little deactivation, between 235 and 500 °C – severe deactivation and at $T > 590$ °C – activation due to a suppression of unselective oxidation of hydrocarbons. The low temperature sulfur tolerance was ascribed to low catalyst activity in SO_2 oxidation to SO_3 with the latter considered to be the main poisoning agent for Ag/Al_2O_3. The authors have evaluated a few regeneration options of which heating to 650 °C in hydrogen-containing lean mixture showed promising results rather than regeneration under oxidizing conditions without H_2. The fastest regeneration technique included heating the catalyst in a rich mixture containing CO and hydrogen.

The results of other research groups [10,11] agree with Breen's results in SO_2 oxidation to SO_3 by NO_2 being the major step in the sulfur poisoning of Ag/Al_2O_3 catalysts. Partial regeneration of the catalyst was observed after heating to 600 °C in a hydrocarbon-containing feed.

In this work we have attempted to reveal the Ag/Al_2O_3 sulfation and regeneration mechanisms, which will allow us to develop an efficient regeneration strategy for the ammonia SCR catalyst in question. Special attention was given to the catalyst operation below 300 °C, since for applications in light-duty diesel vehicles low temperatures are of great importance [10]. The suggested mechanism was supported by DFT calculations. A regeneration strategy using the high temperatures developed during Diesel Particulate Filter (DPF) regeneration in diesel cars was evaluated.

2. Experimental

2.1. Catalyst preparation

Parent γ-alumina (Puralox TH 100/150, $S_{BET} = 150\ m^2/g$) was kindly provided by SASOL. 1–3 wt.% Ag/Al_2O_3 were obtained by incipient wetness impregnation of parent γ-alumina by $AgNO_3$ (Sigma–Aldrich) dissolved in deionized water. After impregnation the catalyst was dried at room temperature overnight and calcined at 550 °C for 4 h in static air. The calcined catalyst was tableted, crushed and sieved to obtain a 0.18–0.35 mm fraction (mesh 80–mesh 45) used in the catalytic tests. A new batch of catalyst was sulfated and used to test every new regeneration recipe.

2.2. Determination of the specific surface area

The specific surface areas (S_{BET}) of the catalysts were measured by N_2-adsorption with a Micromeritics Gemini instrument. Untreated catalysts were measured in powder form and for the catalysts after testing a 0.18–0.35 mm fraction of particles (as in catalytic tests) was used for the BET measurement.

2.3. Catalysis

Temperature-programmed activity tests were carried out in a fixed-bed flow reactor (quartz tube with 4 mm inner diameter) in a temperature programmed mode while the temperature was decreased from 400 °C to 150 °C with a rate of 2 °C/min. Prior to the temperature ramp the catalyst was heated to 470 °C for 30 min in the gas mixture used for the tests. The temperature was controlled using an Eurotherm 2408 temperature controller with a K-type thermocouple. 45 mg of catalyst was diluted with 100 mg of SiC (mesh 60) and placed on a quartz wool bed. The bed height was ~11 mm and the GHSV, calculated using the volume of the pure catalyst was ~110,000 h^{-1}. The gas composition normally contained 500 ppm NO, 520 ppm NH_3, 1200 ppm of H_2, 8.3% O_2, and 7% water balanced with Ar. For sulfur poisoning tests 10 ppm SO_2 was admixed to the feed. Water was dosed by an ISCO 100DM syringe pump through a heated capillary. Reaction products were analyzed by a Thermo Fisher Nicolet 6700 FTIR analyzer, equipped with a 2 m gas cell. Gas capillaries were heated to ~130 °C and the FTIR gas cell to 165 °C to avoid condensation of water and formation of ammonium nitrate.

Conversions were calculated using the following equations:

$$X_{NO_x} = 1 - \frac{C_{NO_x}^{outlet}}{C_{NO_x}^{inlet}} \quad (1)$$

and

$$X_{NH_3} = 1 - \frac{C_{NH_3}^{outlet}}{C_{NH_3}^{inlet}} \quad (2)$$

where X_{NO_x} denotes the conversion of NO_x to N_2 and $C_{NO_x}^{inlet}$ and $C_{NO_x}^{outlet}$ are the NO_x concentrations at the inlet and outlet of the reactor respectively, where:

$$C_{NO_x} = C_{NO} + C_{NO_2} + C_{N_2O} \quad (3)$$

and $C_{NH_3}^{inlet}$ and $C_{NH_3}^{outlet}$ are NH_3 concentrations at the reactor inlet and outlet.

2.4. DFT calculations

The plane wave density functional theory (DFT) code DACAPO was used to calculate the adsorption energies and the gas phase energies of the adsorbates [12]. A plane wave cutoff of 340.15 eV and a density cutoff of 680 eV were used in the calculations. The core electrons were described by Vanderbilt ultrasoft pseudopotentials. The RBPE functional was used for describing the exchange correlation energy [13].

The adsorption energies of the SO_2, SO_3, and SO_4 species were studied over the Ag (1 1 1) terrace and (2 1 1) step surfaces, on a γ-Al_2O_3 model step surface, and two single atom Ag sites.

For the Ag (1 1 1) and (2 1 1) surfaces, we used a $4 \times 4 \times 1$ Monkhorst-Pack **k**-point sampling in the irreducible Brillouin zone. We employed a 3×3 surface cell for the Ag (1 1 1) and 3×1 surface cell for the Ag (2 1 1) surfaces. For the (1 1 1) surface we used a four-layer slab where the two top-most layers were allowed to relax, whereas for the (2 1 1) surfaces we used a slab model with nine layers and the topmost three layers are allowed to relax. In all the model calculations, neighboring slabs were separated by more than 10 Å of vacuum.

For the calculation of γ-Al_2O_3 and the adsorption of different species on γ-Al_2O_3 we also used the DACAPO code with a plane wave cutoff of 340.15 eV and a density cutoff of 680 eV. A $4 \times 4 \times 1$ Monkhorst-Pack **k**-point sampling in the irreducible Brillouin zone was used for γ-Al_2O_3. The γ-Al_2O_3 surface was modeled by a step on a non-spinel γ-Al_2O_3 structure which was derived from bulk γ-Al_2O_3 model in [14]. The cell parameters for the γ-Al_2O_3 model step surface are $a = 8.0680$ Å and $b = 10.0092$ Å and $\alpha = \beta = \gamma = 90°$. For the γ-$Al_2O_3$ surface the bottom two layers were fixed whereas the top-most three layers were allowed to relax. In all the model γ-Al_2O_3 surfaces, the neighboring slabs are separated by more than 10 Å of vacuum.

Single atom Ag sites were constructed by replacing one Al atom for Ag in the alumina step surface and by attaching one Ag atom to the γ-Al_2O_3 step (see Supplementary material for the geometries).

SO_x and HSO_x adsorption energies were calculated relative to gas phase energies of SO_2(g), O_2(g) and H_2(g).

For calculation of desorption temperatures for SO_2 and SO_3 we used the following procedure. Starting from the chemical equation:

$$SO_2 + * \leftrightarrow SO_2*, \quad (4)$$

$$SO_2 + 1/2O_2 + * \leftrightarrow SO_3* \quad (5)$$

where * is the free surface site and SO_x* is the adsorbed species. We can write down the ratio of occupied and free adsorption sites:

$$\frac{\theta_{SO_x}}{\theta^*} = K_{ads}P_{SO_x} = \exp\left(-\frac{\Delta G_{ads}}{kT}\right)P_{SO_x} = \exp\left(\frac{-(\Delta G^{\ominus}_{ads} - kT\ln P_{SO_x})}{kT}\right) \quad (6)$$

We assume that at the desorption temperature the numbers of occupied and free adsorption sites will equal ($\theta_{SO_x} = \theta^*$), which gives:

$$\Delta G^{\ominus}_{ads} - kT\ln P_{SO_x} = 0 \quad (7)$$

or

$$\Delta E_{ads} - \Delta ZPE_{ads} - T\Delta S_{ads} - kT\ln P_{SO_x} = 0 \quad (8)$$

We calculate the ZPE (zero point energy) and the entropy of the SO_x in their adsorbed state and so it is possible to calculate the desorption temperature for a given partial pressure of SO_x:

$$T = \frac{\Delta E_{ads}}{k\ln P_{SO_x} - \Delta S_{gas}} \quad (9)$$

The SO_x entropy and ZPE found for the γ-Al_2O_3 model surface were also used for the single Ag atom sites on the γ-Al_2O_3. Standard entropy values for SO_2 and SO_3 from [15] (neglecting entropy change with temperature) and a partial pressure of SO_x 4×10^{-7} bar (0.4 ppm in Ref. [9]) and partial pressure of O_2 is 0.07 bar [9] were used in the calculations.

3. Results and discussion

3.1. Catalyst choice: stability of Ag/Al_2O_3 and options for the regeneration

3.1.1. The catalyst choice

Temperature dependence of NO_x and NH_3 conversions for the fresh 1–3% Ag/Al_2O_3 catalysts is shown in Fig. 1a and b, respectively. 1% Ag/Al_2O_3 exhibits SCR onset at 130 °C reaching 80% NO_x conversion at 200 °C and leveling NO_x conversion at 90% at $T > 300$ °C. This is in agreement with previous studies [2]. 2% and 3% Ag/Al_2O_3 catalysts demonstrate SCR onset shifted by 7 °C to lower temperatures compared 1%, but lower maximum conversion and generally lower SCR activity at higher temperatures, unlike results of Shimizu and Satsuma [3]. The NH_3 conversion follows the NO_x conversion at $T < 270$–300 °C. At higher temperature NH_3 becomes oxidized and the NH_3 conversion is higher than NO_x conversion. Thus, NH_3 oxidation plays some role in the decrease of high temperature NO_x conversion but this is not the main reason. The reason for observing conversion maxima for 2% and 3% Ag/Al_2O_3 catalysts at 200 °C with subsequent drop in NH_3 and NO_x conversions could be direct oxidation of H_2 by oxygen taking over. As it was shown earlier no NO and NH_3 is converted over an Ag/Al_2O_3 catalyst in the absence of H_2 [16]. Another possible reason is the lack of strong acid sites for NH_3 adsorption in the 2–3% Ag/Al_2O_3 catalysts which is demonstrated in [17].

Noteworthy, the tested catalysts demonstrate very high stability at temperature up to 700 °C which has also been shown in the number of papers on HC-SCR [3,9]. To further check the thermal stability of the 1% Ag/Al_2O_3 catalyst it was subjected to hydrothermal deactivation at 750 °C for 16 h. The activity of the obtained catalyst is reported in Fig. 1a and b as gray dotted lines. The low-temperature conversion is only slightly shifted by 3 °C, whereas at $T > 300$ °C one may observe a decrease in NO_x and NH_3 conversions similar to that observed for catalysts with higher Ag loading. This may indicate sintering of Ag particles leading to the increased unselective oxidation of hydrogen. At the same time, the relatively small decrease in the catalyst specific surface area (S_{BET}) does not indicate any significant change in the alumina support (Table 1).

Contrary to the hydrothermal aging, sulfur poisoning of Ag/Al_2O_3 leads to significant catalyst deactivation. Preliminary experiments on the choice of sulfur poisoning temperature showed no catalyst deactivation with SO_2 in the feed at 500 °C and the most severe deactivation in the temperature range 200–300 °C in very good agreement with the earlier reported results for HC-SCR [8,9]. Therefore, preliminary SO_2 deactivation studies of 1–3% Ag/Al_2O_3 were performed at 200–227 °C and all the following deactivation–regeneration studies of 2% Ag/Al_2O_3 were done at 240–250 °C (Fig. 1c). For the comparison of regeneration methods the SO_2 poisoning was obtained by introducing 10 ppm SO_2 to the SCR feed for 4 h.

Catalytic performance of 1–3% Ag/Al_2O_3 in NO_x SCR after such sulfur treatment at 200–227 °C is shown in Fig. 1d. Lowering deactivation temperature from 250 °C to 200 °C leads to a very small shift of the low-temperature activity within 5 °C, therefore, the temperature difference is not the determining factor for the observed activity difference. 1% Ag/Al_2O_3 was poisoned to the highest degree, whereas higher Ag loading led to better sulfur tolerance with 3% Ag/Al_2O_3 showing the highest NO_x conversion at $T < 300$ °C. It should be noted that after exposure to SO_2 (and even after regeneration of 1% and 2% Ag/Al_2O_3 catalysts at 670 °C) the NH_3 conversion profiles coincided with the NO_x conversion profiles for all tested samples. That indicates quenching of NH_3 unselective oxidation over 1–3% Ag/Al_2O_3 by SO_2. Due to the similarity of NO_x and NH_3 conversion curves for the sulfated catalysts only NO_x conversions will be reported throughout the article.

Sulfation of 2 and 3% Ag/Al_2O_3 leads not only to a shift of the maximum NO_x conversion to higher temperatures but also to an increase to significantly higher values than demonstrated over the fresh catalysts. The shift of the maximum activity of 2% Ag/Al_2O_3 along with "activation" of the catalyst at 227 °C (near the conversion maximum of the fresh catalyst) and at 250 °C can be seen in Fig. 1c. Higher SO_2 exposure leads to a shift of the maximum NO_x conversion to higher temperatures along with deterioration of the low-temperature activity. The activity gain induced by sulfation has been observed earlier and attributed to the redistribution of Ag species [4]. However, as we have observed the decrease of unselective NH_3 oxidation after SO_2 exposure, we suppose the SO_x blocking of sites active in NH_3 and H_2 oxidation to play a major role in the increased NO_x conversion over 2 and 3% Ag/Al_2O_3 catalysts. At the same time SO_2 adsorption increases the alumina acidity which can also play the role for the SCR activity as discussed in a separate publication [17].

Several options for the catalyst regeneration under hydrocarbon (HC) SCR have been suggested in the literature. All of them include heating sulfated Ag/Al_2O_3 in different media – oxidizing [9], hydrogen (or hydrocarbon)-containing lean exhaust [6,8–10] or rich exhaust [6,9].

Heating sulfated 2% Ag/Al_2O_3 to 670 °C for 10 min in the NO_x SCR feed without hydrogen leads only to a small 10 °C shift of T50% to lower temperatures (not shown). Therefore, regeneration of Ag/Al_2O_3 for NO_x SCR by NH_3 without co-feeding hydrogen is ineffective. Thus, regeneration at 670 °C in the reaction gas mixture was used to test the regeneration capability of 1–3% Ag/Al_2O_3 catalysts. Activity of the catalysts regenerated during 40 min is reported in Fig. 1e. All catalysts partially regained the low-temperature activity, however, the high-temperature activity of 3% Ag/Al_2O_3 was

Table 1
Specific surface areas of tested catalysts as measured by BET.

Catalyst	Treatment	S_{BET} (m^2/g)
1% Ag/Al_2O_3	–	142
1% Ag/Al_2O_3	Hydrothermal aging (750 °C, 16 h)	126
2% Ag/Al_2O_3	Catalytic test (w/o deactivation)	130
2% Ag/Al_2O_3	Sulfation and 10 min regen. @ 670 °C	129
2% Ag/Al_2O_3	Sulfation and 80 min regen. @ 670 °C	113
2% Ag/Al_2O_3	30 cycles of 1 h sulfation and 10 min regen. @ 670 °C, followed by heating to 950 °C	121
3% Ag/Al_2O_3	–	141

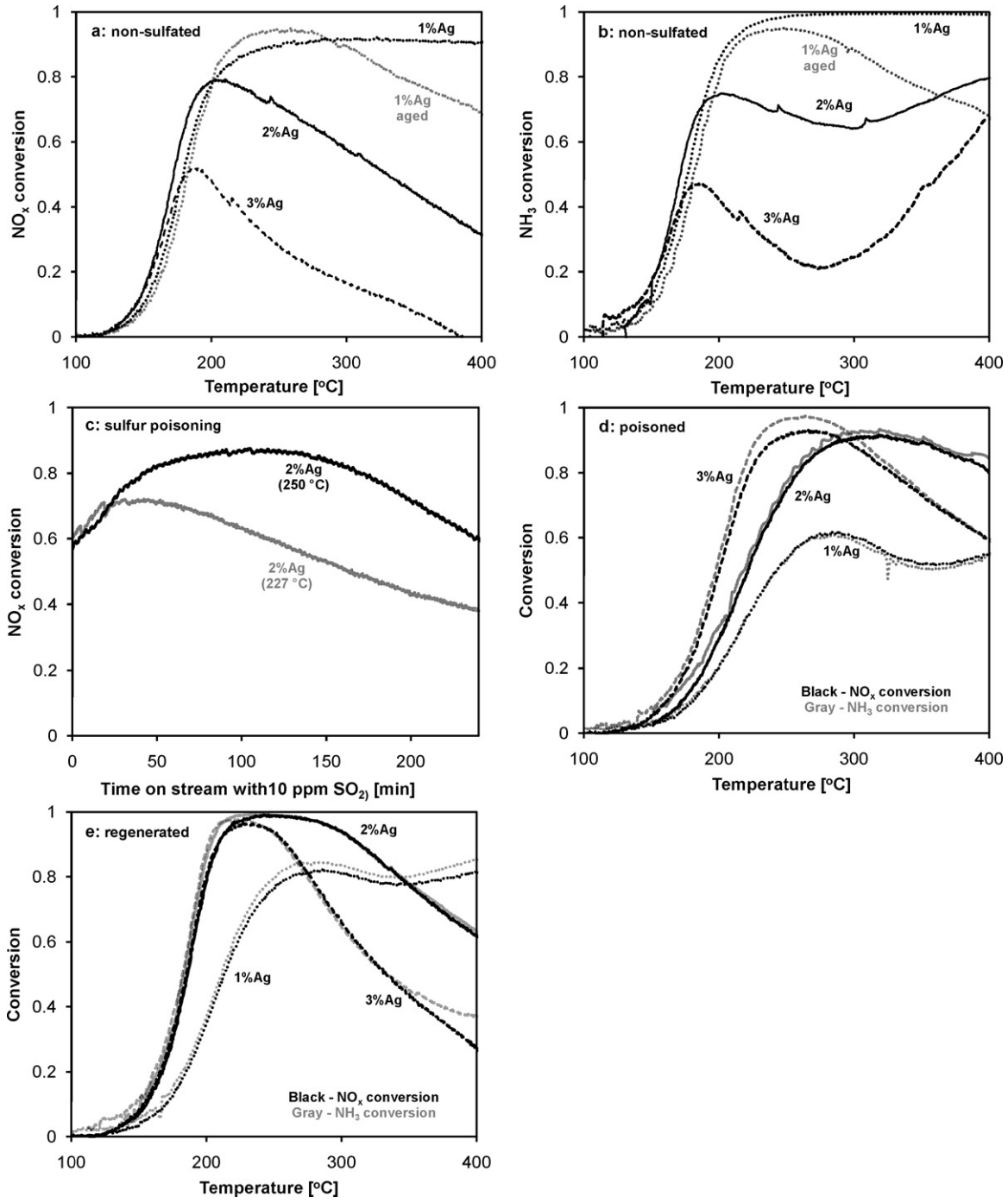

Fig. 1. NO_x (a) and NH_3 (b) conversion profiles obtained over fresh 1–3% Ag/Al_2O_3 (black) and hydrothermally aged 1% Ag/Al_2O_3 (gray dotted) catalysts. (c) Evolution of NO_x conversion at 227 and 250 °C over 2% Ag/Al_2O_3 with 10 ppm SO_2 in the feed. (d) NO_x and NH_3 conversion profiles obtained over sulfur poisoned 1–3% Ag/Al_2O_3 catalysts. (e) NO_x and NH_3 conversion profiles obtained over 1–3% Ag/Al_2O_3 catalysts after 40 min regeneration at 670 °C. Reaction conditions: 500 ppm NO, 520 ppm NH_3, 1200 ppm H_2, 8.3% O_2, 7% H_2O in Ar, GHSV = 110,000 h^{-1}.

decreased compared to the sulfated catalyst. At the same point this catalyst demonstrated a higher conversion of NH_3 compared to NO_x at $T > 350\,^{\circ}C$, indicating NH_3 oxidation. 2% Ag/Al_2O_3 showed the highest NO_x conversion throughout the whole temperature region and will, therefore, be used for the further study. For the simplicity in the text below and the following figures 2% Ag/Al_2O_3 will be referred as Ag/Al_2O_3.

3.1.2. Regeneration options

To simulate regeneration in rich exhaust the catalyst was heated to 670 °C for 1 min with oxygen removed from the feed. The activity following from this rich regeneration is presented in Fig. 2a as a solid line. The profile is significantly shifted to lower temperatures compared to the non-regenerated sample. Another feature is the maximum NO_x conversion (96%), which is now higher than that of both the fresh and the non-regenerated catalysts. Still, regeneration under rich conditions did not allow regaining the low-temperature activity completely.

However, obtaining rich exhaust from diesel engine leads to high fuel consumption and is, therefore, undesirable. Thus, we have preferred relatively fast catalyst regeneration under lean conditions with co-feeding hydrogen. The NO_x conversion profile for Ag/Al_2O_3 regenerated 10 min at 670 °C in the standard NO_x SCR feed (with hydrogen) is shown in Fig. 2a as a dashed line. The catalyst shows the same activity below 200 °C as when regenerated under rich conditions and at higher temperatures even higher conversion (up to 100%). At the same time the surface area of the catalyst regenerated for 10 min is not deteriorated compared to the fresh catalyst (Table 1). This kind of regeneration is very easy to implement in diesel vehicles because it can coincide with regeneration of the DPF, which requires a similar heating strategy.

3.2. Influence of the regeneration time on the catalyst activity

Regeneration time is of high importance for automotive catalysts, as heating the catalyst requires a lot of energy, i.e. fuel to be spent. Influence of the regeneration time (for regeneration under lean conditions with co-feeding hydrogen) on the activity of the regenerated catalyst is shown in Fig. 2b. The value on the *Y*-axis is the shift of temperature for 50% NO_x conversion over the regenerated catalyst relative to the fresh catalyst:

$$T50\%\,\text{shift} = T50\%\,\text{regenerated} - T50\%\,\text{fresh} \quad (10)$$

Zero at the timescale stands for non-regenerated catalyst. Heating to 670 °C for 1 min leads to the shift of *T*50% by 24 °C towards lower temperatures, which is already very good. Heating for 10 min allows us to get 6 °C lower *T*50%, but further treatment at high temperatures does not lead to significant further activation of the catalyst. The best *T*50%, we could get by regenerating Ag/Al_2O_3, is 15 °C higher than *T*50% of the fresh Ag/Al_2O_3. That result is obtained after 40 min of regeneration. Higher regeneration time does not yield better activity but causes loss of the catalyst surface area (Table 1) and is, therefore, undesirable. It is worth noting that we were not able to match the low-temperature activity of the fresh catalyst after regeneration.

3.3. Developing a deactivation–regeneration strategy to mimic automotive catalyst operating conditions

Typical lifecycle of an automotive light-duty Ag/Al_2O_3 NO_x SCR catalyst comprises normal driving, during which the catalyst operates at low temperatures 150–350 °C [10] and is poisoned by sulfur, and regeneration which optimally coincides with regeneration of the DPF. To be more precise, useful vehicle running time according to the modern Euro 5 and Euro 6 standards is 160,000 km [18], and typical intervals between DPF regenerations are 300–900 km (with the modern Volvo D5 light-duty diesel engine as an example) [19], which gives a minimum of 160 catalyst regeneration cycles. Using average fuel consumption of this engine during urban driving (6.7 l/100 km with a manual gearbox), an average diesel fuel density approx. 850 g/l [20], and a maximum allowed sulfur content of 10 ppm in the diesel fuel [21], the total sulfur passed through the catalyst will amount to 91 g or 2.85 mol. Using available data on the volume of monolith catalyst for the mentioned engine (9 l) and the monolith density 2.5 g/in^3 [10], the weight of the washcoat for an automotive catalyst (15% of the total) and the relative weight of the powder catalyst in the washcoat (80%) [22], we get a total of 0.47 g (14.7 mmol) sulfur per gram of powder catalyst during the vehicle lifetime. Therefore, the amount of sulfur per one deactivation cycle will be 83 μmol/g of catalyst, assuming adsorption of all sulfur. In reality, however, not all sulfur will be adsorbed partly due to very high or low temperatures [9].

In our tests we have chosen the scheme involving catalyst poisoning with 10 ppm SO_2 at intermediate temperature of 240 °C for 1 h which gives us a sulfur exposure before regeneration of 65 μmol/g of catalyst, which is close to the theoretical maximum value calculated above. Thus, we will use this protocol as "worst case" scenario.

Fig. 3a and b shows two different ways of testing sulfur tolerance with the same total sulfur exposure (4 h with 10 ppm SO_2, corresponds to 260 μmol/g catalyst) and the same regeneration time, but split by four relatively small regeneration segments in the second case.

The comparison of the catalyst activity after these two tests is given in Fig. 3c. Evidently, the low-temperature activities of the two poisoned catalysts are identical. Different SCR activity at $T > 200\,^{\circ}C$ does not allow us to state that the regenerated catalyst activity observed in Fig. 3c represents "steady state" automotive catalyst activity in both cases. Further testing is needed to reveal "steady state" catalyst activity during sulfation–regeneration cycles.

3.4. Cycling deactivation–regeneration

In order to clarify if the catalyst will be further deactivated after several 1 h. SO_2 poisoning – 10 min regeneration cycles we have carried out 30 deactivation (at 240 °C) – regeneration (at 670 °C) cycles. Evolution of the NO_x and NH_3 conversions during the first 9 cycles of the experiment is shown in Fig. 4.

During the sulfation of the fresh catalyst (first 60 min) NO_x conversion steadily increases. During heating the catalyst to 670 °C the NO_x conversion drops to slightly negative values. According to Eq. (1) in Section 2.3 this is due to a higher NO_x concentration at the reactor outlet than at the inlet. The latter is caused by oxidation of part of ammonia to NO_x at the regeneration temperature which can be seen by the higher conversion of NH_3 compared to NO_x at $T > 500\,^{\circ}C$. To prevent ammonia oxidation in the real life application it is possible to switch off ammonia supply during regeneration without compromising regeneration efficiency.

The NO_x conversion following regeneration is maximal (97%) after the first regeneration and decreases only a little (to 95%) with further regeneration cycles. However, sulfur poisoning of the regenerated sample leads to a decrease in the NO_x conversion at the end of each of the first deactivation cycles. This decrease in NO_x conversion could indicate that during each of these first regenerations the SO_x adsorbed during the preceding deactivation cycle is not completely removed from the catalyst surface. After seven sulfation–regeneration cycles NO_x conversion is stabilized, so each new testing cycle yields the same profile as the previous. Thus, further sulfation and regeneration do not change the catalyst performance.

Integration of the SO_2 signal measured by FTIR during 10th–20th cycles (they are all equal) gives the amount of SO_2 equal to the

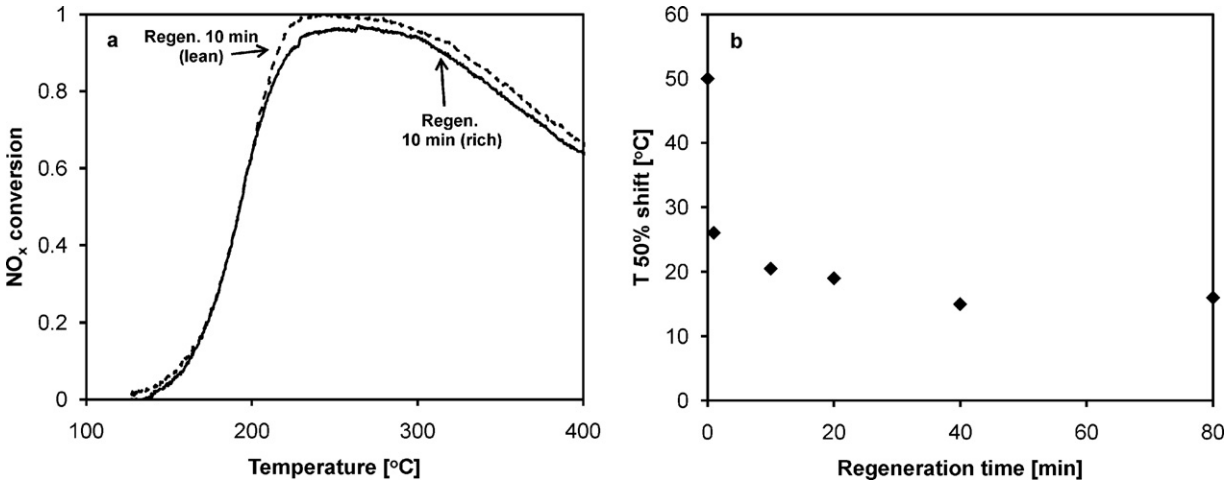

Fig. 2. (a) NO_x conversion profiles obtained over 2% Ag/Al_2O_3 after 10 min regeneration at 670 °C (dashed) and after 1 min regeneration at 670 °C in rich mixture (solid). Reaction conditions: 500 ppm NO, 520 ppm NH_3, 1200 ppm H_2, 8.3% O_2, 7% H_2O in Ar, GHSV = 110,000 h^{-1}. (b) Dependence of shift of temperature of 50% NO_x conversion on the regeneration time. The 0 corresponds to no regeneration.

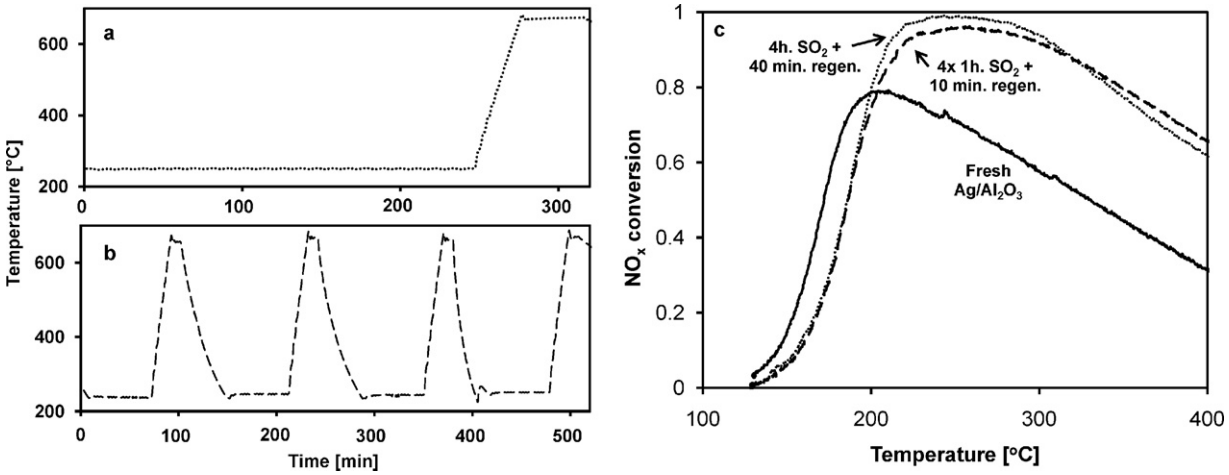

Fig. 3. (a) Temperature profile of 4 h sulfation – 40 min regeneration experiment. (b) Temperature profile of 4 × 1 h sulfation – 10 min regeneration experiment. (c) NO_x conversion profiles obtained over fresh 2% Ag/Al_2O_3 (solid line), 2% Ag/Al_2O_3 after 4 h with 10 ppm SO_2 at 240 °C and 40 min regeneration at 670 °C (dotted line), after 4 cycles 1 h with 10 ppm SO_2 at 240 °C and 10 min regeneration (dashed line).

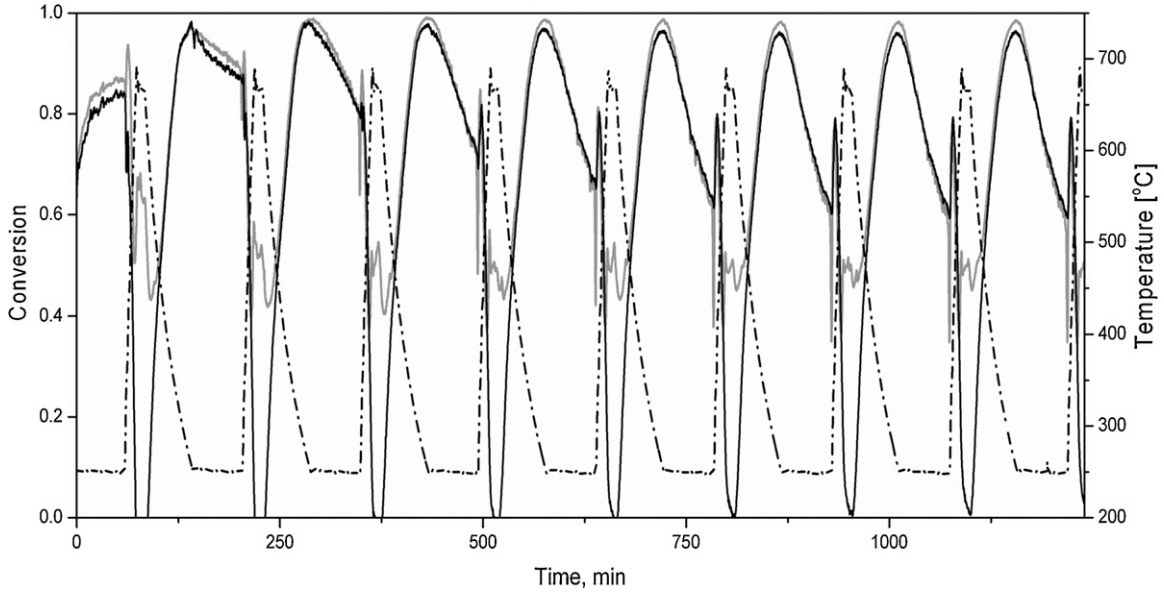

Fig. 4. Evolution of NO_x conversion with time for the first 9 cycles of the long-term stability test of 2% Ag/Al_2O_3. Reaction conditions: 500 ppm NO, 1200 ppm H_2, 8.3% O_2, 7% H_2O in Ar, GHSV = 110,000 h^{-1}. Sulfation with 10 ppm SO_2 for 1 h at 240 °C, regeneration for 10 min at 670 °C.

amount of SO_2 passed through the catalyst during these cycles. Therefore, using FTIR data we can estimate the amount of SO_2, which was accumulated in the catalyst and not desorbed during the first regenerations to be 0.11 mmol/g catalyst.

Our data (not shown) suggests that the SO_2 poisoning effect is cumulative in the range of SO_2 concentrations 0.5–10 ppm, i.e. the catalyst deactivation degree depends only on total SO_2 exposure. Therefore, with the same SO_x exposure between DPF regenerations as in this study real catalyst performance will be high enough even in the end of a sulfation cycle before the next regeneration.

3.5. Mechanism of Ag/Al_2O_3 sulfation and regeneration

The results obtained in the previous Section 3.4 set the ground for a few conclusions regarding the sulfation and regeneration mechanisms for Ag/Al_2O_3 catalysts of hydrogen-assisted NO_x SCR by NH_3.

First of all, some amount of SO_x is not desorbed after regeneration. This amount was estimated in the previous section and is reproducible. At the same time we cannot regenerate the full low-temperature activity of Ag/Al_2O_3, no matter if lean hydrogen-containing or rich mixtures were used for the regeneration. The SCR reaction onset for the sulfated and regenerated catalyst is always shifted to higher temperatures. Therefore, we suppose that a certain type of active sites exists (name it "Type I"), which stand for Ag/Al_2O_3 activity at low temperatures (<200 °C) that are irreversibly poisoned by SO_2 and cannot be regenerated using standard techniques. Taking into account the very low sulfur tolerance of low-loaded Ag/Al_2O_3 [6,7], we can attribute Type I active sites to highly dispersed silver e.g. $Ag^{\delta+}$ atoms or Ag^+ ions [23,24] (see Fig. 5).

SO_x adsorption on the alumina surface (where dispersed silver is localized) blocks these Type I active sites. SO_x can be adsorbed on single-atom Ag sites on the alumina as well as on the neighboring Al atoms. It is impossible to desorb SO_x from the alumina surface by heating the catalyst to 670 °C [25] and, therefore, Type I active sites could not be regenerated.

Another evidence of irreversibly poisoned active sites is the formation of excess of nitrogen dioxide over the fresh catalyst (Fig. 6b, solid line), a catalytic function which is irreversibly poisoned by SO_2 and cannot be regenerated (Fig. 6b, dotted line). Therefore, we also attribute the increased NO oxidation capacity to Type I active sites.

However, the possibility of regeneration of the most of the SCR activity of Ag/Al_2O_3 hints on the existence of "Type II" active sites. As they are more abundant in more SO_2 tolerant high-loaded Ag/Al_2O_3 [7] we attribute them to the surface of Ag nanoparticles. It has been shown that it is possible to desorb SO_2 from the Ag surface at temperatures near 600 °C [25]. Thus, we assume that sulfation and regeneration of these Type II active sites determines the SCR activity of Ag/Al_2O_3 with sulfur-containing fuel in diesel vehicles. According to the SCR mechanism suggested in [16] these Type II species are also capable of oxidizing NO to NO_2 which further reacts with NH_3 over alumina. However, Type II sites are less active which leads to the deficit of NO_2 and prevents observing it in the gas phase when NH_3 is present.

Our assumption about the existence and function of Type I active sites can be verified by the following. As follows from the SO_2 TPD profiles in Refs. [11,25], it is possible to desorb SO_x from alumina surface at ca. 1000 °C. Of course, the alumina will undergo partial restructuring at this temperature [26] accompanied by the formation of the α-Al_2O_3 phase, which will partially ruin the catalyst. However, this may help to test the principle.

The results of heating of sulfated Ag/Al_2O_3 to 950 °C in the SCR gas mixture with further immediate cooling are shown in Fig. 6a and b as dashed lines. By removing SO_x from the alumina surface (observed by FTIR) we were able to regain SCR onset at the same temperature as for the fresh Ag/Al_2O_3 (Fig. 6a). At the same time we were able to regenerate excessive NO_2 production (Fig. 6b) which was impossible to get by any kind of regeneration at lower temperature. Still, the maximum activity of the catalyst was lower than that of the fresh catalyst resembling the activity of 3% Ag/Al_2O_3 (Fig. 1a). The specific surface area of the catalyst regenerated at 950 °C did not change significantly compared to the fresh sample (Table 1), therefore, it is rather sintering of Ag particles which caused a drop in the maximum activity. Thus, we consider possibility of regenerating low temperature activity as an evidence for the existence of several types of active sites in Ag/Al_2O_3 as was previously stated for HC-SCR Ag/Al_2O_3 catalysts [27].

The fact that SO_x irreversibly adsorbed on the alumina surface does not hinder that the SCR reaction can be explained if we assume that Ag species participate in the oxidation of NO to NO_2 and the alumina facilitates further reaction of NO, NO_2 and NH_3 according to the "Fast SCR" mechanism [28]. Since "Fast SCR" occurs over a number of acidic surfaces, sulfated alumina should catalyze SCR as well if SO_x-free Ag surface is left to oxidize NO.

3.6. Evaluation of the proposed sulfation and regeneration mechanism of Ag/Al_2O_3 by DFT

Adsorption energies of SO_2, SO_3, and SO_4 for the most energetically favorable adsorption geometries for different adsorption sites are summarized in Table 2 and the corresponding geometries for the γ-alumina model step surface are shown in Fig. 7. It should be noted that SO_x can be adsorbed on the γ-alumina in different configurations with similar energies and only the lowest energies (strongest adsorption) are shown. The DFT calculation shows that the SO_x adsorbs strongly on the step sites which is expected from the low coordination of these sites and the steric freedom available at the step sites [29–31]. At the same time the surface step is representative of small 1–3 nm nanoparticles containing mostly under-coordinated surface atoms [32].

Two trends can be identified from these values. First global trend is that all types of SO_x bind significantly stronger to the alumina surface than the metal surface. The adsorption sites also include single Ag sites at the alumina surface with Ag atom built in the surface substituting Al is binding SO_x most strongly (see Supplementary material for the exact site geometry). This can be explained by a thermodynamically unfavorable defect structure of this site. Secondly, the oxidation of SO_2 to SO_3 is thermodynamically favorable, with subsequent poisoning of the catalyst surface by the resulting SO_3. This has been suggested in Ref. [9] and probably involves reaction with NO_2 [11]. SO_2 alone cannot be adsorbed on the studied metallic Ag surfaces under reaction conditions and SO_x can, thus, only poison the alumina support or single Ag sites on this surface.

The calculated desorption temperatures (Table 2) are low but the order, at which regeneration of Type II (Ag surface) and Type I (highly dispersed Ag on the alumina) occurs is in agreement with the mechanism of Ag/Al_2O_3 poisoning and regeneration suggested in Section 3.5. The difference between calculated and experimental desorption temperatures [11,25] might indicate the formation of bulk silver sulfate [7,33,34].

At the same time addition of hydrogen significantly enhances catalyst regeneration i.e. removal of SO_x which could be due to the formation of the correspondent HSO_x species with their subsequent desorption. Table 3 shows the energies of the HSO_x species in the gas phase and adsorbed on the most energetically favorable sites. According to the given numbers, the formation of HSO_x is highly favorable on Ag (2 1 1). As the adsorption energies of the HSO_x species with respect to the gas phase species H_2SO_3 (g) and H_2SO_4 (g) are very small they are easily desorbed. The formation of HSO_x is not favorable on the model γ-Al_2O_3 step surface and at the site with Ag built into the γ-Al_2O_3 model step surface. Thus,

Table 2
Adsorption energies and desorption temperatures of SO_x for the most energetically favorable adsorption geometries in case of different adsorption sites.

	Type II (metallic Ag)				Type I (dispersed Ag)					
	Ag (1 1 1)		Ag (2 1 1)		γ-Al_2O_3		Ag built in the γ-Al_2O_3 surface		Ag on the step of γ-Al_2O_3	
	E_{ads} (eV)	T_{des} (K)	E_{ads} (eV)	T_{des} (K)	E_{ads} (eV)	T_{des} (K)	E_{ads} (eV)	T_{des} (K)	E_{ads} (eV)	T_{des} (K)
SO_2	Not adsorbed	–	−0.26	81	−1.43	558	−2.06	791	−1.29	506
SO_3	−1.61	390	−1.82	458	−2.66	630	−3.34	781	−2.64	625
SO_4	−2.65	454	−2.97	597	−1.15	222	−1.77	331	−3.14	572

Table 3
Energies of HSO_x species in the gas phase and adsorbed on the most energetically favorable adsorption sites.

Energy[a] (eV)	HSO_2	HSO_3	H_2SO_3	HSO_4	H_2SO_4
Gas phase	0.21	−0.75	−2.15	−1.48	−3.39
Adsorbed on γ-Al_2O_3	Dissociates	−2.84	−2.18	−3.16	Dissociates
Adsorbed on Ag built in the γ-Al_2O_3	Dissociates	−4.10	−3.38	−3.61	Dissociates
Adsorbed on Ag (2 1 1)	0.02	−2.56	−2.22	−3.94	−3.57

[a] Energy of the HSO_x species is given with respect to SO_2 (g), O_2 (g) and H_2 (g).

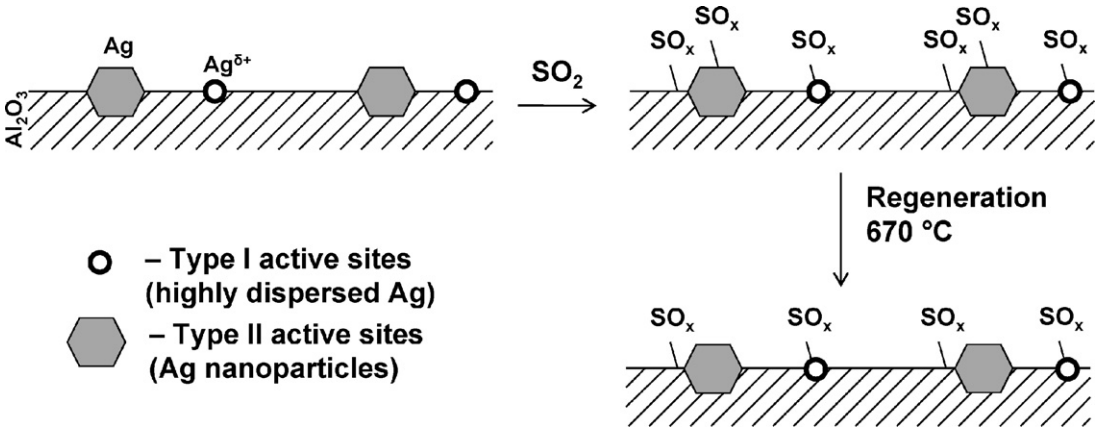

Fig. 5. The scheme of Ag/Al_2O_3 sulfation and regeneration.

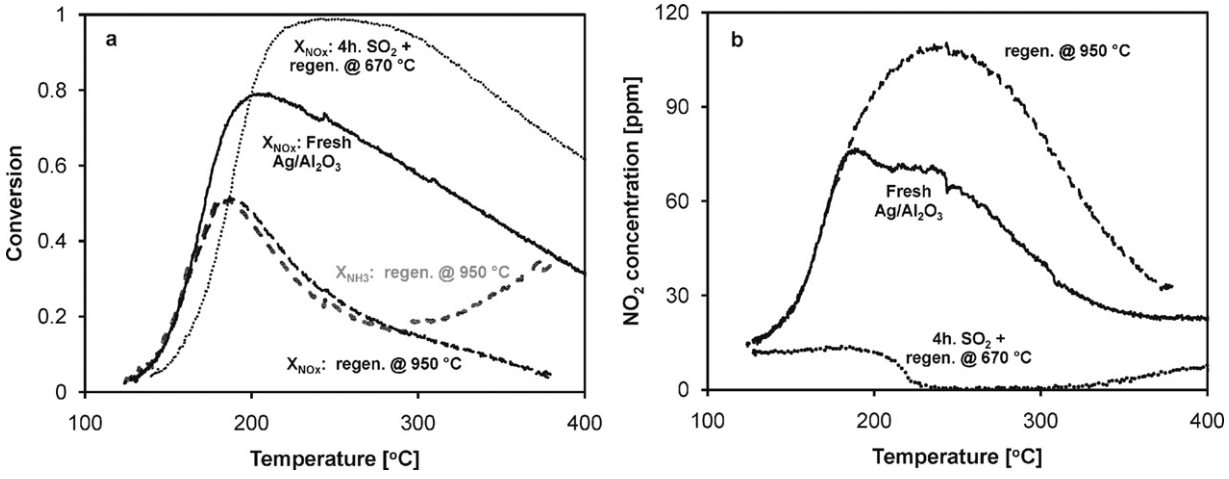

Fig. 6. (a) NO_x conversion profiles obtained over fresh 2% Ag/Al_2O_3 (solid line), 2% Ag/Al_2O_3 after 4 h with 10 ppm SO_2 at 240 °C, followed by 40 min regeneration at 670 °C (dotted line) and after additional regeneration at 950 °C (dashed line). (b) Temperature dependence of NO_2 concentration at the reactor outlet obtained over fresh 2% Ag/Al_2O_3 (solid line), 2% Ag/Al_2O_3 after 4 h with 10 ppm SO_2 at 240 °C, followed by 40 min regeneration at 670 °C (dotted line) and after additional regeneration at 950 °C (dashed line). Reaction conditions: 500 ppm NO, 520 ppm NH_3, 1200 ppm H_2, 8.3% O_2, 7% H_2O in Ar, GHSV = 110,000 h^{-1}.

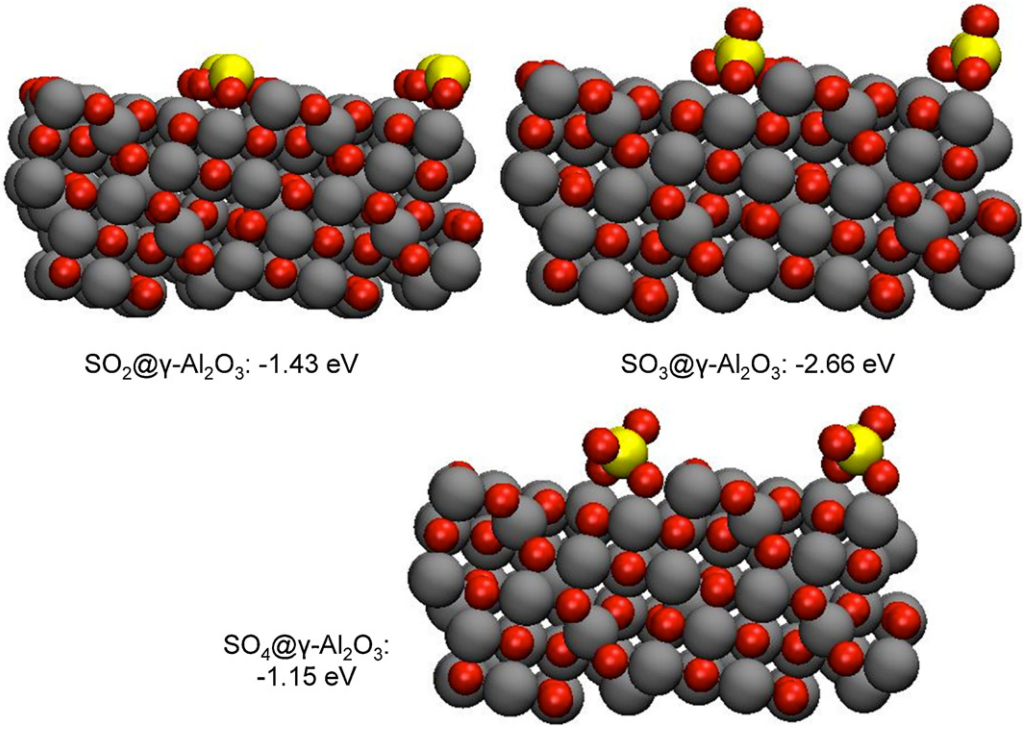

Fig. 7. The most energetically favorable adsorption geometries for adsorption of SO_2, SO_3, and SO_4 on the γ-Al_2O_3 model surface (with corresponding adsorption energies).

presence of H_2 will promote the desorption of SO_x species from the Ag (2 1 1) surface via formation of H_2SO_3 (g) and H_2SO_4 (g) but not for γ-Al_2O_3 surface and the single Ag sites on the γ-Al_2O_3 surface.

4. Conclusions

Sulfur tolerance and regeneration options of 2% Ag/γ-Al_2O_3 catalyst for H_2-assisted NO_x SCR by NH_3 have been tested. The catalyst has medium sulfur tolerance at low temperatures, however a good capability of regeneration. This regeneration should include heating to 650–700 °C for 10–20 min, provided the SCR gas feed is unchanged (ammonia may be removed) and hydrogen is co-fed. Regeneration of Ag/Al_2O_3 without oxygen (rich mixture) leads to essentially the same effect, but requires less time.

Heating to 650–700 °C does not allow full regeneration of low-temperature activity and does not allow recovery of NO_2 formation over Ag/Al_2O_3 in the course of SCR.

During the long-term tests with cycling poisoning–regeneration periods the catalyst activity is regenerated during each regeneration cycle, but at least for the first 6–7 cycles sulfur species are accumulated on the catalyst. Presumably, SO_x is removed from Ag, but not from the alumina surface during standard regeneration, which allows us to make a conclusion on the existence of different active sites in Ag/Al_2O_3, namely finely dispersed Ag ions and Ag nanoparticles.

Acknowledgement

This work was supported by the Danish Council for Strategic Research through grant 09-067233.

Appendix A. Supplementary data

Supplementary data associated with this article can be found, in the online version, at doi:10.1016/j.apcatb.2012.01.002.

References

[1] T.V. Johnson, Int. J. Engine Res. 10 (2009) 275–285.
[2] M. Richter, R. Fricke, R. Eckelt, Catal. Lett. 94 (2004) 115–118.
[3] K.-I. Shimizu, A. Satsuma, Appl. Catal. B 77 (2007) 202–205.
[4] A. Abe, N. Aoyama, S. Sumiya, N. Kakuta, K. Yoshida, Catal. Lett. 51 (1998) 5–9.
[5] H. Kannisto, X. Karatzas, J. Edvardsson, L.J. Pettersson, H.H. Ingelsten, Appl. Catal. B 104 (2011) 74–83.
[6] F.C. Meunier, J.R.H. Ross, Appl. Catal. B 24 (2000) 23–32.
[7] P.W. Park, C.L. Boyer, Appl. Catal. B 59 (2005) 27–34.
[8] S. Satokawa, K.-I. Yamaseki, H. Uchida, Appl. Catal. B 34 (2001) 299–306.
[9] J.P. Breen, R. Burch, C. Hardacre, C.J. Hill, B. Krutzsch, B. Bandl-Konrad, E. Jobson, L. Cider, P.G. Blakeman, L.J. Peace, M.V. Twigg, M. Preis, M. Gottschling, Appl. Catal. B 70 (2007) 36–44.
[10] F. Klingstedt, K. Eränen, L.-E. Lindfors, S. Andersson, L. Cider, C. Landberg, E. Jobson, L. Eriksson, T. Ilkenhans, D. Webster, Top. Catal. 30/31 (2004) 27–30.
[11] Q. Ma, Y. Liu, H. He, J. Phys. Chem. A 112 (2008) 6630–6635.
[12] B. Hammer, L.B. Hansen, J.K. Nørskov, Phys. Rev. B 59 (1999) 7413–7421.
[13] E. Mènendez-Proupin, G. Gutièrrez, Phys. Rev. B 72 (2005) 35116–35119.
[14] M. Digne, P. Sautet, P. Raybaud, P. Euzen, H. Toulhoat, J. Catal. 226 (2004) 54–68.
[15] M.W. Chase Jr., NIST-JANAF Themochemical Tables, fourth edition, J. Phys. Chem. Ref. Data, Monograph 9, 1998, 1–1951.
[16] D.E. Doronkin, S., Fogel, S., Tamm, L., Olsson, T.S., Khan, T., Bligaard, P. Gabrielsson, S. Dahl, Appl. Catal. B, in press, doi:10.1016/j.apcatb.2011.11.042.
[17] S. Fogel, D.E. Doronkin, P. Gabrielsson, S. Dahl, Manuscript in preparation.
[18] Regulation (EC) No. 715/2007 of the European Parliament and of the Council of 20 June 2007, Official Journal of the European Union, (29.6.2007), L 171/1–L 171/16.
[19] VOLVO S80 Instruktionsbok Web Edition http://esd.volvocars.com/site/owners-information/MY11/S80/PDF/S80_owners_manual_MY11_SE_tp11740.pdf (accessed June 2011).
[20] G.M. Wallace, European Diesel Fuel – A Review of Changes in Product Quality 1986–1989, Preprint Archive of the ACS Division of Fuel Chemistry 35 (4) (1990) 1080–1099.
[21] Directive 2009/30/EC of the European Parliament and of the Council of 23 April 2009, Official Journal of the European Union, (5.6.2009), L 140/88–L 140/113.
[22] L. Olsson, H. Sjövall, R.J. Blint, Appl. Catal. B 81 (2008) 203–217.
[23] A. Sultana, M. Haneda, T. Fujitani, H. Hamada, Catal. Lett. 114 (2007) 96–102.
[24] K.-I. Shimizu, J.H.Y. Shibata, A. Satsuma, T. Hattori, Appl. Catal. B 30 (2001) 151–162.
[25] Q. Wu, H. Gao, H. He, J. Phys. Chem. B 110 (2006) 8320–8324.
[26] I. Levin, D. Brandon, J. Am. Ceram. Soc. 81 (1998) 1995–2012.

[27] R. Burch, J.P. Breen, F.C. Meunier, Appl. Catal. B 39 (2002) 283–303.
[28] T.C. Brüggemann, D.G. Vlachos, F.J. Keil, J. Catal. 283 (2011) 178–191.
[29] B. Hammer, J.K. Nørskov, Adv. Catal. 45 (2000) 71–129.
[30] B. Hammer, O.H. Nielsen, J.K. Nørskov, Catal. Lett. 46 (1997) 31–35.
[31] Á. Logadóttir, J.K. Nørskov, J. Catal. 220 (2003) 273–279.
[32] T.V.W. Janssens, B.S. Clausen, B. Hvolbæk, H. Falsig, C.H. Christensen, T. Bligaard, J.K. Nørskov, Top. Catal. 44 (2007) 15–26.
[33] N. Jagtap, S.B. Umbarkar, P. Miquel, P. Granger, M.K. Dongare, Appl. Catal. B 90 (2009) 416–425.
[34] B. Kartheuser, B.K. Hodnett, Alfredo Riva, G. Centi, H. Matralis, M. Ruwet, P. Grange, N. Passarini, Ind. Eng. Chem. Res. 30 (1991) 2105–2113.